arXiv:1405.5403v2 [cond-mat.stat-mech] 24 Jun 2014

Interacting Elastic Lattice Polymers: a Study of the Free-Energy of Globular Rings

M. Baiesi and E. Orlandini
Department of Physics and Astronomy, University of Padua, Via Marzolo 8, I-35131 Padova, Italy and INFN, Sezione di Padova, Via Marzolo 8, I-35131 Padova, Italy

We introduce and implement a Monte Carlo scheme to study the equilibrium statistics of polymers in the globular phase. It is based on a model of "interacting elastic lattice polymers" and allows a sufficiently good sampling of long and compact configurations, an essential prerequisite to study the scaling behavior of free energies. By simulating interacting self-avoiding rings at several temperatures in the collapsed phase, we estimate both the bulk and the surface free energy. Moreover from the corresponding estimate of the entropic exponent $\alpha - 2$ we provide evidence that, unlike for swollen and Θ-point rings, the hyperscaling relation is not satisfied for globular rings.

PACS numbers: 64.60.De 36.20.-r, 05.10.Ln, 64.60.an,

I. INTRODUCTION

It is well known that diluted polymers in bad solvent conditions may undergo a conformational transition from the swollen (extended) phase to a globular one [1–3]. In the last decades this so-called *collapse transition* has been the subject of numerous experimental and theoretical studies that have been essentially focused either on the swollen phase or on the nature and scaling properties of the collapse (Θ) transition [4–8]. On the other hand very little is known about polymers in the globular phase [9–15], despite the study of their statistics can help in understanding the conformational and thermodynamic properties of more complex forms of compact polymers such as proteins in native states.

If one is mainly interested in the scaling behavior of either metric or thermodynamics observables (including critical exponents) of collapsing polymers, a good model to consider is the class of N-site interacting self-avoiding walks (ISAWs), namely, non self-intersecting walks of N sites on Bravais lattices with an attractive interaction between adjacent non-bonded sites. Indeed, by tuning this attraction in terms of an effective temperature $T = 1/\beta$, ISAWs display a collapse transition towards a globular phase whose thermodynamics is governed, in the limit of large N, by the scaling behavior of the partition function [9–15]

$$Z_N(\beta) \sim \mu^N e^{-\sigma N^{(d-1)/d}} N^\theta \left(1 + BN^{-\Delta} \cdots\right). \quad (1)$$

(such structure is also supported by theoretical results for partially directed ISAWs [16, 17] and for dense polymers [18, 19]). In (1) the connective constant μ and the amplitude B of the correction to scaling are model dependent quantities and function of β, whereas the (entropic) exponent θ is a universal (i.e. model independent) critical exponent whose value depends only on dimension (d) and on polymer topology (for instance linear, circular, knotted etc). Note in (1) the presence of the term $e^{-\sigma N^{(d-1)/d}}$ that describes the surface penalty contribution ($\sigma > 0$ for $\beta > \beta_\Theta$) related to the higher free energy acquired by the monomers exposed to the solvent [9, 12–15]. The presence of this surface renders the asymptotic analysis of the thermodynamics of globular polymers more complicated than that for dense polymers, at least for two reasons: First, the presence of the additional unknown parameter σ increases the complexity of the analysis of the scaling law (1). Second, there is strong numerical evidence that the surface generates strong corrections to scaling when linear polymers are considered [14]. The reason is that configurations with one or both ends on the surface of the globule surface have different entropic exponents with respect to those where both ends are in the interior of the globule, the latter become asymptotically relevant only for long chains. This effect has been observed for $d = 2$ globules [14] and should be even more pronounced for globular polymers in $d = 3$, where the surface/volume ratio is larger than in two dimensions. A way to get around this problem consists for instance in looking at globular rings.

Scaling laws such as (1) are usually studied numerically by N-varying (grand-canonical) Monte Carlo approaches [20–23]. An example is the so called BFACF algorithm [20, 21] (from the initials of the authors), a set of local moves including the deletion/addition of a few monomers along the walk. Being ergodic within the class of rings with a given knot type [24], this algorithm has also been extensively used to study the effect of topological constraints on the asymptotic properties of knotted rings in the swollen phase [25]. However, it is known that its straightforward application to the globular phase fails to reproduce the N-varying statistics with a controlled average number of monomers $\langle N \rangle$ if N is sufficiently large [26, 27], a condition to achieve for studying the scaling law (1) properly.

Here we introduce a stable numerical scheme to study the large N behavior of globular polymers. This is applied on a model of interacting polymer that from now on we refer to as an *interacting elastic lattice polymer* (IELP). The IELP can be seen as an extension of the elastic lattice polymer (ELP), a model that has been introduced to study dynamical properties of linear polymers [28, 29] and more recently extended to investigate the equilibrium properties of rings in the swollen phase [30]. Briefly (see the next section for a better definition of the model) an M-monomer IELP is an ISAW

where locally the self-avoiding condition can be partially relaxed by allowing some consecutive monomers to condense on the same lattice site. In this respect the M monomers of an IELP are elastically stored along an ISAW backbone with fluctuating length $N \leq M$. This additional degree of freedom, not present in the standard ISAW model, can then be tuned to better stabilize the average length $\langle N \rangle$ when N-varying algorithms are used in stochastic sampling. Moreover, by restricting the sampling to circular IELPs (rings), the aforementioned finite-size corrections, due to the positions of the polymer ends with respect to the globule surface, can be avoided. Finally, by looking at the asymptotic behavior of the equilibrium averaged stored length density

$$\rho_M = \frac{M - \langle N \rangle}{M}, \tag{2}$$

we have access to the full scaling law (1) and we are able to estimate its parameters in the globular phase.

This paper is organized as follows: In Section II we introduce the IELP model and its asymptotic behavior in the globular phase. In particular we show how to extract information on the μ, σ, and θ exponents by extrapolating the average stored length density ρ_M for large M values. In Section III we describe the N-varying Monte Carlo algorithm used to sample closed IELPs on the hypercubic lattice and its implementation on a Multiple Markov Chains scheme, an additional stochastic procedure known to increase the mobility of the sampling for compact configurations. In Section IV we show the results obtained for collapsed rings, ending with some conclusions in Section V.

II. THE IELP MODEL FOR GLOBULAR POLYMERS

A commonly used model to study numerically the polymer collapse transition is the ISAW, namely a SAW augmented with an attractive energy $-E$ equal to the number of contacts (non-bonded pairs of nearest-neighbors sites of the SAW).

In the grand-canonical ensemble the large N behavior of ISAWs is governed by the singularities of the generating function

$$G(K, \beta) = \sum_N K^N Z_N(\beta) \tag{3}$$

where K is the *step fugacity*, β the inverse of the temperature and

$$Z_N(\beta) = \sum_E e^{-\beta E} C_N(E) \tag{4}$$

is the canonical partition function associated with the number of N-sites ISAWs with energy E, $C_N(E)$. The singularities of (3) develop as $K \to K_c(\beta)^-$ and Monte Carlo algorithms based on the BFACF moves must bring the value of K as close as possible to $K_c(\beta) = 1/\mu(\beta)$ to get a good statistics of configurations with large N.

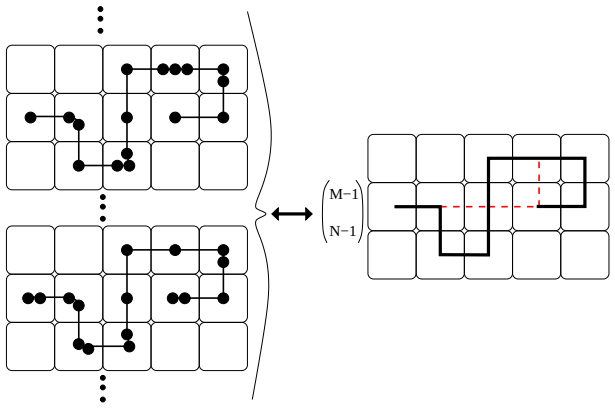

FIG. 1. Example of ELPs with $M = 16$ monomers and $N = 10$ sites (left) sharing the N-sites SAW silhouette (right). Dashed lines represent the energetic contacts associated to that configuration.

Unfortunately a straightforward application of the BFACF algorithm in the globular phase meets a difficulty. Indeed, due to the presence of the surface term $\sim e^{-\sigma N^{2/3}}$ in (1) of Z_N, the grand-canonical average $\langle N \rangle = \Sigma_N N K^N Z_N / \Sigma_N K^N Z_N$ does not grow continuously to $+\infty$ as $K \to K_c(\beta)^-$ but instead jumps discontinuously to infinity right at $K = K_c$, making the sampling of long walks quite unrealistic [26].

In order to allow the number of sites N to fluctuate and grow in a rather controlled way we introduce the IELP model, an extension of the ELP model for SAWs in which self-attracting interaction is taken into account. As in the ELP model, the idea is to accommodate $M \geq N$ monomers on an underlying N-site SAW silhouette drawn on a lattice. To maintain the connectivity constraint of a polymer chain, at least one monomer resides in each site of the underlying N-site SAW and only consecutive monomers can share the same lattice site (see Fig. 1).

Certainly one could sample IELPs by updating the position of all M monomers within the lattice [31]. However, this level of detail is not necessary when the energy function depends only on the N-sites ISAW silhouette: in this case it is sufficient to sample directly the ISAWs backbone with rates that take into account the degeneracy of each ISAW configuration. Since for each N-site ISAW there are $\binom{M-1}{N-1}$ possible IELPs, the total weight associated with an IELP configuration with M monomers, N lattice sites and E contacts, is given by

$$W = K^N e^{-\beta E} \binom{M-1}{N-1}. \tag{5}$$

By summing over all possible values of E and N compatible with M we obtain the generating function of IELPs

with M monomers

$$Z^{IELP}(M,\beta) = \sum_{N\leq M} \binom{M-1}{N-1} K^N Z_N(\beta). \quad (6)$$

Note that, when M and K are both kept fixed, the number of sites N oscillates around an average $\langle N\rangle_{K,M,\beta}$ that scales linearly with M, with fluctuations of the order of $\sqrt{M}$. This property, as we will show below, is very helpful in sampling long walks undergoing a Θ-collapse.

A second advantage in sampling IELPs is the possibility of estimating $\mu(\beta)$, $\sigma(\beta)$ and θ by computing the asymptotic of the mean stored length density (2) within a saddle-point approximation [30]. To show this we first notice that, by defining $\omega(\beta) \equiv \mu(\beta)K$ and substituting the scaling (1) in (6), the average $\langle N\rangle$ can be computed by using the relation

$$\langle N\rangle(\beta) = \omega\frac{\partial}{\partial\omega}\log Z^{IELP}(M,\beta). \quad (7)$$

If the partition function of ISAWs were simply $Z_N(\beta) = \mu(\beta)^N$, one would get the exact expression $N_\infty(\beta) = \langle N\rangle(\beta) = M\omega(\beta)/[1+\omega(\beta)]$ [30]. Thus, by using the change of variable $N = xN_\infty$, the saddle-point approximation of the partition function becomes

$$Z^{IELP}(M,\beta) \sim (1+\omega)^M \sqrt{\frac{\omega M}{2\pi}} \int_{-\infty}^{+\infty} e^{M\omega F(x)} dx \quad (8)$$

with

$$F(x) = -\frac{(x-1)^2}{2} + \frac{1}{M\omega}\left[-\sigma(xN_\infty)^{2/3} + \theta\ln(xN_\infty) + \ln\left(1+B(xN_\infty)^{-\Delta}\right)\right] \quad (9)$$

Denoting by $\bar{x}$ the location of the maximum of $F(x)$, the approximation gives

$$Z^{IELP}(M,\beta) \sim (1+\omega)^M \frac{e^{M\omega F(\bar{x})}}{\sqrt{|F''(\bar{x})|}} \quad (10)$$

Since in the large M limit

$$|F''(\bar{x})| = 1 + \mathcal{O}\left(\frac{1}{M}\right), \quad (11)$$

$$\bar{x} = 1 + \mathcal{O}\left(\frac{1}{M}\right), \quad (12)$$

we get

$$M\omega F(\bar{x}) = -\sigma N_\infty^{2/3} + \theta\ln N_\infty + \ln\left(1+B(N_\infty)^{-\Delta}\right). \quad (13)$$

We then have

$$\begin{aligned}\langle N\rangle = \omega\frac{\partial}{\partial\omega}\ln Z^{IELP}(M,\beta) &= N_\infty\left[1 - \frac{2\sigma}{3}\frac{N_\infty^{-1/3}}{1+\omega} + \frac{\theta}{N_\infty}\frac{1}{1+\omega} - \frac{B\Delta N_\infty^{-\Delta-1}}{1+BN_\infty^{-\Delta}}\frac{1}{1+\omega}\right] \\ &= N_\infty\left[1 - \frac{2\sigma}{3}\frac{N_\infty^{-1/3}}{1+\omega} + \frac{\theta}{M\omega} - \frac{B\Delta}{M\omega}\left(\frac{1+\omega}{M\omega}\right)^{\Delta}\left(1+BN_\infty^{-\Delta}\right)^{-1}\right] \quad (14)\end{aligned}$$

from which we get the scaling of the density $\rho_M(\beta) = 1 - \langle N\rangle/M$ to order $1/M^{1+\Delta}$,

$$\rho_M(\beta) = \rho_\infty(\beta)\left[1 + \frac{2\sigma(\beta)}{3}\left(\frac{\omega(\beta)}{1+\omega(\beta)}\right)^{2/3}\frac{1}{M^{1/3}} - \frac{\theta}{M} + B(\beta)\Delta\left(\frac{\omega(\beta)}{1+\omega(\beta)}\right)^{-\Delta}\frac{1}{M^{1+\Delta}}\right] \quad (15)$$

where

$$\rho_\infty(\beta) = 1 - \frac{N_\infty}{M} = \frac{1}{1+\omega(\beta)}. \quad (16)$$

We stress that at high temperature the surface term is not present and the leading term is the one proportional to the exponent θ, which scales as $1/M$ [30]. On the other hand, in the globular phase the σ term is $\sim 1/M^{1/3}$: in the limit of large M it dominates the entropic one, which now acts as a (weak) correction to scaling.

III. MONTE CARLO ALGORITHM FOR IELP

Since the Monte Carlo algorithm for IELPs is based on the BFACF moves, its ergodicity is a direct consequence of the one already proven for BFACF [32]. The Monte Carlo scheme samples ISAWs configurations according to the statistical weight (5) of IELPs; it is then enough to require that the rate of jump R_{AB} from a configuration A to a configuration B satisfies the detailed balance condition $W_A R_{AB} = W_B R_{BA}$. From Eq. (5) we get

$$\frac{R_{AB}}{R_{BA}} = \frac{W_B}{W_A} \quad (17)$$

$$= K^{N_B-N_A} e^{-\beta(E_B-E_A)} \binom{M-1}{N_B-1} / \binom{M-1}{N_A-1}$$
$$= K^{N_B-N_A} e^{-\beta(E_B-E_A)} \frac{(N_A-1)!(M-N_A)!}{(N_B-1)!(M-N_B)!}.$$

We now specialize the discussion to M-monomers circular IELPs, whose underlying silhouette is given by a N-steps self-avoiding polygon (SAP) on a d-dimensional hyper-cubic lattice. Note that in this case the periodicity in monomer labeling requires $N+1 \equiv 1$ with the number of monomers equal to the number of steps. The BFACF moves that need some care in their implementation are those changing the number N of monomers. These are based on the addition/removal of a crankshaft bulge: in such a motif a site i along the chain is a nearest neighbor of site $i+3$ and, together with $i+1$ and $i+2$, they form a unit square on the hypercubic lattice (see a $d=2$ example in Fig. 2).

The addition/removal of two sites connects the ensemble of SAPs with $N_A = N$ sites to that of SAPs with $N_B = N_A + 2$ sites. Accordingly, equation (18) simplifies to

$$\frac{R_{AB}}{R_{BA}} = K^2 e^{-\beta(E_B-E_A)} \frac{(N-1)!(M-N)!}{(N+1)!(M-N-2)!}$$
$$= K^2 e^{-\beta(E_B-E_A)} \frac{(M-N)(M-N-1)}{(N+1)N} \quad (18)$$

In practice a local update $A \to B$ that proposes the addition of two monomers is implemented by choosing, with uniform probability $P_A^{\rm ind} = 1/N$, one of the N bonds of polygon A. Then one of the $2d-2$ possible directions orthogonal to the chosen bond, $(i, i+1)$, is picked up with probability $P_A^{\rm dir} = 1/(2d-2)$.

The reverse update $B \to A$ is implemented accordingly by choosing a bond of the polygon B with probability $P_B^{\rm ind} = 1/(N+2)$. By calling $\mathcal{A}_{AB}$ and $\mathcal{A}_{BA}$ the acceptance probability of the direct ($A \to B$) and reverse ($B \to A$) moves respectively, the jump rates R_{AB} and R_{BA} can be written as

$$R_{AB} = f_{AB} P_A^{\rm ind} P_A^{\rm dir} \mathcal{A}_{AB} = \frac{f_{AB}}{2d-2} \frac{1}{N} \mathcal{A}_{AB}$$
$$R_{BA} = f_{BA} P_B^{\rm ind} \mathcal{A}_{BA} = f_{BA} \frac{1}{N+2} \mathcal{A}_{BA} \quad (19)$$

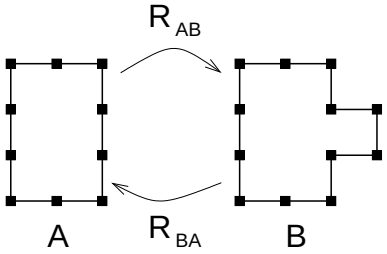

FIG. 2. Example of a proposed move (and its inverse) that transforms locally an N-site configuration A to an $(N+2)$-site configuration B.

where f_{AB} and f_{BA} are the frequencies with which the direct and reverse moves are proposed, respectively. These frequencies can be chosen to satisfy the detailed balance (18). By choosing $f_{AB} = 2d-2$ and $f_{BA} = 1$ we get

$$R_{AB} = \frac{1}{N} \mathcal{A}_{AB}$$
$$R_{BA} = \frac{1}{N+2} \mathcal{A}_{BA}. \quad (20)$$

With this choice the acceptance probabilities become

$$\frac{\mathcal{A}_{AB}}{\mathcal{A}_{BA}} = \frac{N}{N+2} \frac{R_{AB}}{R_{BA}}$$
$$= \frac{N}{N+2} K^2 e^{-\beta(E_B-E_A)} \frac{(M-N)(M-N-1)}{(N+1)N}$$
$$\equiv K^2 e^{-\beta(E_B-E_A)} q(M,N) \quad (21)$$

where we have defined the ratio

$$q(M,N) = \frac{(M-N)(M-N-1)}{(N+1)(N+2)}. \quad (22)$$

Note that $q(M,N) \le 1$ for $N \ge (M-2)/2$ and $q(M,N) > 1$ otherwise.

In the spirit of a Metropolis criterion, the idea is to maximize both $\mathcal{A}_{AB}$ and $\mathcal{A}_{BA}$ compatibly with the above constraint on $q(M,N)$. Ideally, one of the two should be equal to 1. The following acceptance rates of the proposed move $N \to N+2$ and $N \to N-2$ satisfy the above requirements for any value of N:

$$\mathcal{A}(E_A, N \to E_B, N+2) = \min\{1, K^2\} \times \min\{1, q(M,N)\} \times \min\{1, e^{-\beta(E_B-E_A)}\} \quad (23)$$

$$\mathcal{A}(E_B, N \to E_A, N-2) = \min\{1, K^{-2}\} \times \min\{1, q^{-1}(M,N-2)\} \times \min\{1, e^{-\beta(E_A-E_B)}\}. \quad (24)$$

Hence, for a d-dimensional hyper-cubic lattice, when the frequency of proposed moves that increase the number of steps from N to $N+2$, f_{AB}, is $2d-2$ times the frequency of the reverse moves (f_{BA}), we can apply the filters (23)-(24) to accept them. For an efficient implementation of the algorithm once, say, the move $N \to N+2$ is proposed, it is more convenient to pass first the filter equal to $\min\{1, K^2\} \min\{1, q(M,N)\}$ and then, after the self-avoidance test is passed, accept the move with probability equal to $\min\{1, e^{-\beta(E_B-E_A)}\}$.

In addition to the N-varying moves the Monte Carlo scheme provides local corner flips [32] and two-point pivot moves [32], the latter being essential to sample rings with arbitrary topology.

The algorithm just described designs a Markov Chain on the space of IELPs with fixed parameters β and M. Several runs at different values of M are then necessary to span a broad range of density values at fixed β. An efficient way to get several simulations with different M

at once can be obtained by embedding the above algorithm in a sampling scheme where several Markov chains at different Ms run in parallel, and swaps of configurations between contiguous (in M) Markov chains are performed stochastically. This super Markov chain is known as *Multiple Markov Chains* and in the past has been proved to be very effective in increasing the sampling efficiency [7, 33, 34].

By considering (5) one can determine the acceptance ratio of configurations swapping between two Markov chains respectively of parameters M and M': since β and K are fixed, the only relevant term in (5) is the factorial and the acceptance probability of the swap move $A = \{(M,N)\&(M',N')\} \to B = \{(M,N')\&(M',N)\}$ reduces to

$$\mathcal{A}_{AB} = \min\left\{1, \frac{(M-N)!(M'-N')!}{(M-N')!(M'-N)!}\right\}. \qquad (25)$$

If $M' > M$ this equation can be written as

$$\mathcal{A}_{AB} = \min\left\{1, \prod_{i=0}^{M'-M-1} \frac{M'-N'-i}{M'-N-i}\right\} \qquad (26)$$

Since each term of the product is larger than 1 for $N > N'$, a swap that move the longer configuration to higher values of M is always accepted.

For multiple Markov chains at different β's, the swapping of configurations between two contiguous (in β space) Markov chain is likely to be accepted if there is a non negligible overlap between the energy distributions sampled by the two Markov chains. Here the interacting Markov chains are taken at different Ms and a good acceptance rate of swaps between two neighboring chains is expected if there is a non negligible overlap of the corresponding N distributions. Since the dispersion in the Ns sampled is $\sim \sqrt{M}$, the spacing between subsequent values of M should also scale as $\sim \sqrt{M}$. With this choice of M the swapping moves should occur quite frequently, allowing a good mobility of the sampled configuration in the space of M values and hence decreasing the correlation times between in the stochastic sampling (See Fig. 3).

IV. RESULTS

Simulations of circular IELP on the cubic lattice are based on the sampling scheme described in the previous section with $K = 1$, i.e. $\omega = \mu$. By fixing β we run in parallel 46 Markov chains, each with a given value of M from a minimum $M_{\min} = 100$ up to a maximum $M_{\max} = 1000$. As explained in section II, the asymptotic behavior of the average stored length density $\rho_M(\beta)$ can be exploited to investigate the scaling properties of the free energy of globular rings. To test the validity of the approach, let us first consider the scaling of $\rho_M(\beta)$ in the swollen phase. In this case $\sigma = 0$ in (1) and the leading term in (15) is proportional to θ and goes as $1/M$.

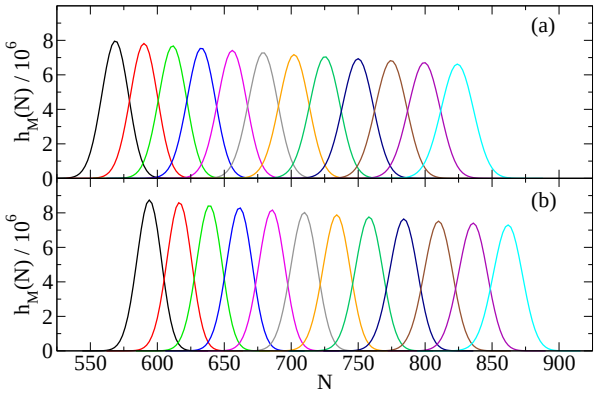

FIG. 3. (Color online) Some of the sampled length distributions for inverse temperature (a) $\beta = 0$ (swollen phase) and (b) $\beta = 0.5$ (collapsed phase). The twelve curves are for different M values, ranging from $M = 690$ (left) to $M = 1000$ (right). The similar overlaps between contiguous distributions are obtained by choosing a spacing between the corresponding M's that scales as $\sqrt{M}$.

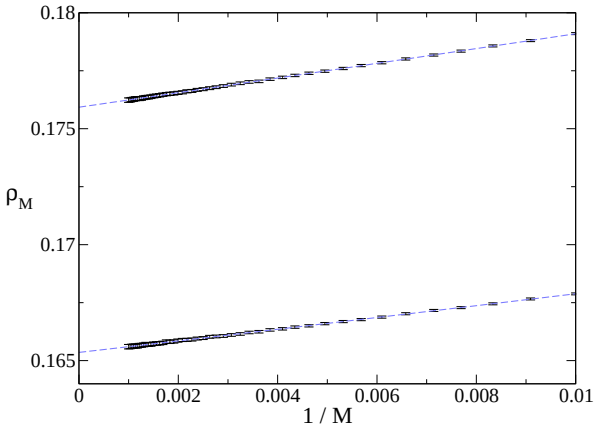

FIG. 4. (Color online) Mean stored length density vs $1/M$ for $\beta = 0$ (top) and $\beta = 0.269$ (bottom). The dashed lines are fits based on (15) with $\sigma = 0$.

Figure 4 shows the scaling behavior of $\rho_M(0)$ as a function of $1/M$ for rings on the cubic lattice. The data converges linearly to an intercept ρ_∞, as expected. By fitting the data with $\Delta = 1/2$ we get the estimates $\rho_\infty(0) \simeq 0.161253$ and $\theta \simeq -1.759$. Given that $\rho_\infty(\beta) = 1/[1+\mu(\beta)]$ and that in rings θ is usually denoted by $\alpha - 2$, we finally get

$$\mu(0) = 4.68412(15), \qquad \alpha = 0.241(22). \qquad (27)$$

These estimates are, within error bars, compatible with the ones obtained in previous studies on the scaling properties of self-avoiding polygons [30, 32]. We perform a similar analysis at the Θ-point ($\beta = 0.269$ [22, 35])) where the surface correction is still absent. The data are also reported in Figure 4 and by fitting them using (15)

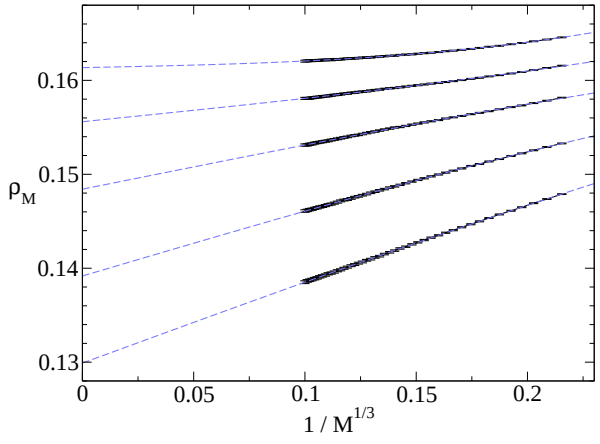

FIG. 5. (Color online) Mean stored length density vs $1/M^{1/3}$ for (from top to bottom) the values of $\beta = 0.32$, 0.36, 0.4, 0.45, and 0.5. The dashed lines are fits based on (15) with $B = 0$.

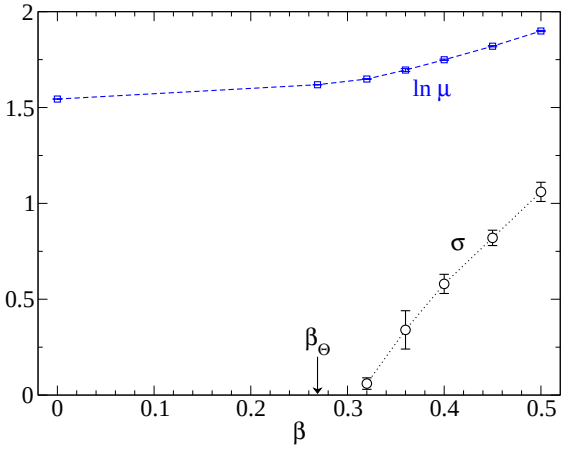

FIG. 6. (Color online) Estimate of the bulk ($\log \mu$) and surface σ free energy contributions at various inverse temperatures β.

with $\Delta = 1/2$ and $\sigma = 0$ we find

$$\mu(0.269) = 5.04762(22), \qquad \alpha = 0.528(31). \tag{28}$$

The estimate of α is more complicated than in the swollen phase due to the presence of logarithmic corrections [36] but the value we find agrees, within error bars, with the mean field value $\alpha = 1/2$ that, in $d = 3$, is supposed to be exact.

We now focus on the scaling properties of globular rings by considering values of $\beta > \beta_\Theta = 0.269$ [22]. In this case the surface free energy term proportional to σ is not negligible and the leading term in (15) should scale as $1/M^{1/3}$. This is confirmed in Figure 5 where, by plotting the data $\rho_M(\beta)$ as a function of $1/M^{1/3}$ a linear behavior occurs for sufficiently large values of M and β. The linear extrapolation of these data at $1/M^{1/3} \to 0$ would give an estimate of $\rho_\infty(\beta)$, the slope of the linear approximation of the curves an estimate of $\sigma(\beta)$ while their curvature furnishes an estimate of θ. Since finite-size effects are present in our data, one should in principle include into the non-linear fit the correction to scaling that depends on B and Δ. However, these two additional unknown parameters would destabilize the fit. We decided instead to proceed as follows: we partitioned the data into three groups according to the M values. In the first group the data with the largest ten values of M are excluded, in the second group are excluded points with the five largest and the five smallest Ms, while the third one excluded the ten smallest Ms. The third group, the most asymptotic one, has been used to estimate $\mu(\beta)$, $\sigma(\beta)$, and θ while the estimates from the other two groups are used to estimate the error bars. In Table I we listed the estimates of $\mu(\beta)$, $\sigma(\beta)$ and $\theta(\beta)$ for a wide values of β in the globular phase. For comparison also the estimates in the swollen phase and at the Θ point have been included.

We first notice that both $\log \mu(\beta)$ and $\sigma(\beta)$ in the globular phase increase with β (see Figure 6) and, deep inside the phase the dependence is linear in β. Since $\log \mu(\beta)$ is proportional to the bulk free energy per monomer $f(\beta)$ of the model, the linear behavior is expected by simple rigorous bounds on $f(\beta)$ (see for example [35]). The linear behavior of $\sigma(\beta)$ can be explained in a similar way by noticing that, in the large β limit, the statistics of the globular phase is dominated by almost "spherical" configurations with surface area of the order of $CN^{2/3}$. This gives a bound on the surface free energy $\sigma(\beta)$ of the order of βC.

Finally the estimates of the entropic exponent α for rings are reported in the last column of Table I and plotted in Fig. 7 for the three sets of data grouped as explained before (we recall that the estimates at $\beta = 0$ and $\beta = \beta_\Theta$ are obtained by using (15) with $\sigma = 0$ and $\Delta = 1/2$). In addition, from the figure it is readily seen that the hyperscaling relation $2 - \alpha = \nu d$ [2, 37] is confirmed both in the swollen phase ($\beta = 0$), where $\nu \approx 0.58797(7)$ [38] and at the Θ point, where $\nu = 1/2$. In the above relation ν is the critical exponent governing the scaling behavior of the average extension of the polymer, and $d = 3$.

In the globular phase ($\nu = 1/d$) the value of α is not

Phase	β	μ	σ	α
swollen	0	4.68412(15)		0.241(22)
Θ-point	0.269	5.04762(22)		0.528(31)
globular	0.32	5.20(1)	0.06(3)	0.8(2)
	0.36	5.45(4)	0.34(10)	2.4(9)
	0.4	5.75(2)	0.58(5)	2.8(6)
	0.45	6.17(2)	0.82(4)	2.5(3)
	0.5	6.68(2)	1.06(5)	2.1(4)

TABLE I. Numerical estimates of μ, σ and α obtained by fitting the data of Figs. 5 and 4 with Eq. (15).

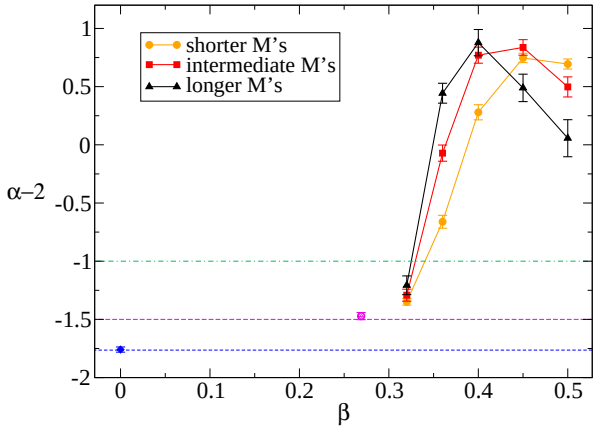

FIG. 7. (Color online) Estimates of the entropic exponent $\alpha-2$ as a function of the inverse temperatures β. The three sets of data for $\beta > 0.3$ show how the estimates of α change by taking more and more asymptotic data. The dashed horizontal lines refer to the hyperscaling values $-\nu d$ expected respectively for rings in the swollen phase and at the Θ-point. The dot-dashed horizontal line refers to the value that one would expect from hyperscaling in the collapsed phase.

know from the theory and, as far as we know, there are no numerical results supporting the hyperscaling relation $\alpha - 2 = -1$. The plot in Figure 7 shows for $\beta > \beta_\Theta$ an initially steep increase of $\alpha - 2$ followed by an unstable behavior deep in the globular phase. While the sharp increase just above the Θ point is a good indication of a single value of α characterizing the globular phase, the actual estimate of this value seems to fluctuate widely between $\alpha = 2$ and $\alpha = 2.7$. This is probably due either to the fact that the sampling at high values of β is not robust and reliable enough or that the neglected correction proportional to B in (15) is important in this region for the values of M considered. More investigations are needed to clarify this issue. On the other hand, by focusing on the crossings formed by the three sets of estimates one observe that, as M increases, the β values of the crossings shift towards the Θ point and correspondingly the α exponents goes closer to a value between 2.7 and 3.0. Despite the important degree of uncertainty in the estimates of α, we can say that, unlike in the swollen phase and at the Θ point, the hyperscaling relation is not valid for globular polymers.

V. CONCLUSIONS

In this paper we have introduced and implemented a Monte Carlo scheme to study the scaling properties of N-steps interacting polymers on the cubic lattice. The sampling scheme is based essentially on the N-varying BFACF moves acting on a class of self-attracting rings that we refer as IELPs. These are chains of M monomers that locally could fold into the same lattice site and hence that can accumulate their total length $M \geq N$ along their N-steps backbone. If the interaction energy coincides with that of the backbone, however, it is not necessary to simulate the moves of the M-monomer IELPs, it is just sufficient to sample N-step configurations with a reweighting term that takes into account the multiplicity of the possible rearrangements of M monomers in N sites. Unlike the standard grand-canonical algorithms, this scheme bounds from above the number of steps N by M, preventing the uncontrolled growth of the average $\langle N \rangle$ during the sampling, a problem that severely affects the N-varying sampling of globular configurations.

By looking at the asymptotic properties of the stored length density $\rho_M(\beta)$ as a function of the inverse temperature β we have been able to study the scaling behavior of the free energy of the interacting SAP model for several values of β, from the swollen phase down to the globular phase, passing through the Θ point. To test the validity of our algorithm, we first estimated the bulk free energy $\log \mu(\beta)$ and the entropic exponent $\alpha - 2$ of the model at $\beta = 0$ and $\beta = \beta_\Theta$, finding a good agreement with previous results. In the so far unexplored globular phase, in addition to the bulk free energy $\log(\mu)$ we gave an estimate of the surface free energy $\sigma(\beta)$. Finally, by looking at the entropic exponent $\alpha - 2$ we furnish good evidence that, unlike in the swollen phase and at the Θ point, the hyperscaling relation $\alpha - 2 = -\nu d$ does not hold for the class of collapsed globular rings.

The Monte Carlo scheme based on IELPs should be particularly useful to study globular rings of fixed knot type [30]. It would then be interesting to apply this sampling scheme to investigate the role of topology in the scaling properties of the free energy of globular knotted rings.

ACKNOWLEDGMENTS

We thank E. Carlon and A. Stella for useful discussions. We acknowledge financial support from the Italian Ministry of Education (Grant PRIN 2010HXAW77).

[1] P.-G. de Gennes, *Scaling concepts in Polymer Physics* (Cornell University Press, Ithaca, New York, 1979).
[2] C. Vanderzande, *Lattice models of Polymers* (Cambridge University Press, Cambridge, 1998).
[3] E. J. Janse van Rensburg, *Statistical Mechanics of Interacting Walks, Polygons, Animals and Vesicles* (Oxford University Press, Oxford, 2000).

[4] B. Duplantier and H. Saleur, Phys. Rev. Lett. **59**, 539 (1987).
[5] F. Seno and A. L. Stella, J. Physique **49**, 739 (1988).
[6] P. Grassberger and R. Hegger, J. Phys. I France **5**, 597 (1995).
[7] M. Tesi, E. J. Janse van Rensburg, E. Orlandini, and S. G. Whittington, J. Stat. Phys. **82**, 155 (1996).
[8] K. Iwata, Macromol. **22**, 3702 (1989).
[9] A. L. Owczarek, T. Prellberg, and R. Brak, Phys. Rev. Lett. **70**, 951 (1993).
[10] B. Duplantier, Phys. Rev. Lett. **71**, 4274 (1993).
[11] A. L. Owczarek, T. Prellberg, and R. Brak, Phys. Rev. Lett. **71**, 4275 (1993).
[12] R. Brak, A. L. Owczarek, and T. Prellberg, J. Phys. A. **26**, 4565 (1993).
[13] P. Grassberger and H. P. Hsu, Phys. Rev. E **65**, 031807 (2002).
[14] M. Baiesi, E. Orlandini, and A. L. Stella, Phys. Rev. Lett. **96**, 040602 (2006).
[15] M. Baiesi, E. Orlandini, and A. L. Stella, Phys. Rev. Lett. **99**, 058301 (2007).
[16] R. Brak, A. J. Guttmann, and S. Whittington, J. Phys. A: Math. Gen. **25**, 2437 (1992).
[17] G. B. Nguyen and N. Pétrélis, J. Stat. Phys. **151**, 1099 (2013).
[18] B. Duplantier and H. Saleur, Nucl. Phys. B **290 [FS20]**, 291 (1987).
[19] B. Duplantier and F. David, J. Stat. Phys. **51**, 327 (1988).
[20] B. Berg and D. Foester, Phys. Lett. B **106**, 323 (1981).
[21] C. A. de Carvalho and S. Caracciolo, J. Physique **44**, 323 (1983).
[22] P. Grassberger, Phys. Rev. E **56**, 3682 (1997).
[23] A. Rechnitzer and E. J. Janse van Rensburg, J. Phys. A: Math. Gen. **41**, 442002 (2008).
[24] E. J. Janse van Rensburg and S. G. Whittington, J. Phys. A: Math. Gen. **24**, 5553 (1991).
[25] E. Orlandini, M. Tesi, E. J. Janse van Rensburg, and S. G. Whittington, J. Phys. A: Math. Gen. **31**, 5953 (1998).
[26] B. Marcone, E. Orlandini, A. L. Stella, and F. Zonta, Phys. Rev. E **75**, 041105 (2007).
[27] M. Baiesi, E. Orlandini, A. L. Stella, and F. Zonta, Phys. Rev. Lett. **106**, 258301 (2011).
[28] A. van Heukelum and G. T. Barkema, J. Chem. Phys. **119**, 8197 (2003).
[29] J. K. Wolterink, G. T. Barkema, and D. Panja, Phys. Rev. Lett. **96**, 208301 (2006).
[30] M. Baiesi, G. T. Barkema, and E. Carlon, Phys. Rev. E **81**, 061801 (2010).
[31] R. D. Schram, G. T. Barkema, and H. Schiessel, J. Chem. Phys. **138**, 224901 (2013).
[32] N. Madras and G. Slade, *The Self-Avoiding Walk* (Birkhäuser, Berlin, 1993).
[33] C. J. Meyer, in *Computing Science and Statistics: Proceedings of the 23rd Symposium on the Interface*, edited by E. M. Keramides (Interface Foundation, Fairfax Station, Virginia, 1991) pp. 156–163.
[34] E. Orlandini, Numerical Methods for Polymeric Systems, edited by S. G. Whittington, IMA Volumes in Mathematics and Its Application **102**, 33 (1998).
[35] M. Tesi, E. J. Janse van Rensburg, E. Orlandini, and S. G. Whittington, J. Phys. A: Math. Gen. **29**, 2451 (1996).
[36] B. Duplantier, J. Physique **43**, 991 (1982).
[37] B. Duplantier, Phys. Rev. Lett. **57**, 941 (1986).
[38] N. Clisby, Phys. Rev. Lett. **104**, 055702 (2010).